Fariñas, JC.; Moreno, R.; Pérez, A.; García, MA.; García-Hernández, M.; Salvador Moya, MD.; Borrell Tomás, MA. (2018). Microwave-assisted solution synthesis, microwave sintering and magnetic properties of cobalt ferrite. Journal of the European Ceramic Society. 38(5):2360-2368. https://doi.org/10.1016/j.jeurceramsoc.2017.12.052

Microwave-assisted solution synthesis, microwave sintering and magnetic properties of cobalt ferrite

J.C. Fariñas[a,*], R. Moreno[a], A. Pérez[a], M.A. García[a], M. García-Hernández[b], M.D. Salvador[c], A. Borrell[c]

[a] *Instituto de Cerámica y Vidrio (CSIC), Campus de Cantoblanco, 28049 Madrid, Spain*

[b] *Instituto de Ciencia de Materiales de Madrid (CSIC), Campus de Cantoblanco, 28049 Madrid, Spain*

[c] *Instituto de Tecnología de Materiales, Universitat Politècnica de València, 46022 Valencia, Spain*

*Corresponding author.

E-mail address: jcfarinas@icv.csic.es (J.C. Fariñas).

ABSTRACT

A simple, soft, and fast microwave-assisted hydrothermal method was used for the preparation of nanocrystalline cobalt ferrite powders from commercially-available $Fe(NO_3)_3{\cdot}9H_2O$, $Co(NO_3)_2{\cdot}6H_2O$, ammonium hydroxide, and tetrapropylammonium hydroxide (TPAH). The synthesis was conducted in a sealed-vessel microwave reactor specifically designed for synthetic applications, and the resulting products were characterized by XRD, FE-SEM, TEM, and HR-TEM. After a systematic study of the influence of the microwave variables (temperature, reaction time and nature of the bases) highly crystalline $CoFe_2O_4$ nanoparticles with a high uniformity in morphology and size, were directly obtained by heating at 190°C for 20 min using the base TPAH. Dense ceramics of cobalt ferrite were prepared by non-conventional, microwave sintering of synthesized nanopowders at temperatures of 850-900ºC. The magnetic properties of both the nanopowders and the sintered specimens were determined in order to establish their feasibility as a permanent magnet.

Keywords: Microwave-assisted solution synthesis; Microwave sintering; Magnetic properties; Cobalt ferrite

1. Introduction

Cobalt ferrite ($CoFe_2O_4$) is a magnetic oxide with inverse spinel structure that exhibits moderate saturation magnetization ($M_S \approx 70$ emu/g at 300 K) and high coercivity, besides great physical and chemical stability [1]. Therefore, $CoFe_2O_4$ has been widely used for video tape and digital recording media [2], magnetic resonance contrast agent [3], magnetically induced hyperthermia for targeted treatments [4], sensors and actuators [5,6], etc. This material exhibits other interesting properties such as magneto-elastic effect [7] and photomagnetism, with variations of the magnetic properties upon visible light illumination with potential uses for magneto-optic transductors in information technologies [8].

It is well known that nanoparticles exhibit different properties than bulk materials with the same composition due to surface size and proximity effects. This nanoscale effect provides a method to tune the properties of the materials for specific applications. In the case of magnetic nanoparticles, the monodomain regime and superparamagnetic effects allows to change the coercivity of the material several orders of magnitude by controlling the particle size. Moreover, the photomagnetism of $CoFe_2O_4$ results strongly enhanced for nanoparticles smaller than 17 nm [8]. Since the properties of the nanoparticles of $CoFe_2O_4$ are strongly influenced by their composition, microstructure and size, which depend on the preparation method, many efforts have been devoted to develop synthesis routes capable to produce nanoparticles with a small size dispersion and controlled morphology.

A large number of preparation methods of cobalt ferrite have been reported in the literature, such as standard solid-state ceramic processing [9,10], seeded-growth thermal decomposition [3], complexometric synthesis [11,12], auto-combustion method [13], microemulsion process [14], sol-gel [15], coprecipitation [16,17], and hydrothermal [18,19], continuous hydrothermal [20], supercritical hydrothermal [21] and solvothermal [22,23] methods. However, these methods often require long times, tedious procedures, multiple step reactions, precise pH control, special working conditions, and the addition of stabilizing or chelating agents. To overcome these shortcomings, an alternative method for the preparation of cobalt ferrite should still be explored.

Microwave irradiation as a heating source has been successfully developed for a number of chemical approaches to produce organic and inorganic solid-state compounds [24-26]. In a microwave system, heating arises from either dipole rotation or ion migration induced by the microwave field, which

subsequently generates rapid, simultaneous and homogeneous nucleation, fast supersaturation, and short crystallization time. Consequently, compared with conventional methods, microwave irradiation has the advantages of rapid volumetric heating, high reaction rates, very short reaction times, production of uniform small particles with a narrow particle size distribution and high purity, great selectivity and high product yield. As a quick, simple, clean and energy efficient method, microwave-assisted synthesis has become widely used for the preparation of inorganic nanocrystals [27,28], including cobalt ferrite [29-33]. Therefore, an alternative route to control the composition, microstructure and crystal size of $CoFe_2O_4$ powders can be offered by the microwave-assisted synthesis. In addition, the use of $CoFe_2O_4$ nanoparticles requires the development of synthesis methods that can be scaled-up with reduced economic costs but also capable to control precisely the particle size and morphology, which can be achieved with this technique.

Komarneni *et al.* [29] prepared cobalt ferrite for the first time by microwave-assisted synthesis. The reaction was performed in a microwave oven system controlled by pressure for 120 min. Kim *et al.* [30] studied the influence of both temperature and time, and they found that the crystallinity of the products improved with the two variables. They also compared the microwave-assisted synthesis with the conventional hydrothermal method, and they obtained that the conventional method requires a relatively higher temperature and longer reaction time than the microwave method to promote crystallization. No measurements of the magnetic properties were made in any of the two papers. Ibrahim *et al.* [31] synthesized nano-sized single phase cobalt ferrite by a polyol method using both conventional and microwave heating techniques. No data about temperature were reported. Microwave heating technique produced particles in the range of 10 nm. The saturation magnetization value of the microwave produced sample (94.8 emu/g) was close to the reported for $CoFe_2O_4$ (≈90 emu/g), and these values were larger than that of the samples prepared by conventional heating technique. This behaviour was attributed by the authors to the presence of undetectable very small clusters of metallic Co(0) and/or Fe(0) originated by the reduction of few metallic ions by the ethylene glycol solvent, which is a reducing agent, during the reaction. The magnitudes of the coercivity of the prepared samples are in all cases much smaller than that reported for cobalt ferrite, whereby the material will be soft magnetic material. Briefly, the sample obtained by using microwave heating technique exhibits significant characteristics such as the smallest particle size, the highest saturation magnetization value and also low coercivity. Bensebaa *et al.* [32] also use a polyol method with microwave heating at 160°C for 60 min under reflux conditions to obtain a single-phase cobalt ferrite, although a relatively small amount of the acetate (from raw materials) and polyol molecules remains adsorbed on the surface of the nanoparticles,

contributing about 16% of the weight. The magnetic response in DC fields was typical for an assembly of single-domain particles, and the measured saturation magnetization was slightly larger than the bulk value, probably due to the presence of small amounts of unreacted Co and Fe. AC magnetization data indicated the presence of magnetic interactions between the nanoparticles. Baruwati *et al.* [33] prepared monodisperse $CoFe_2O_4$ nanoparticles at a water-toluene interface using oleic acid as the dispersing agent under conventional hydrothermal conditions at 250°C for 1 and 2 h, as well as under microwave hydrothermal conditions at 160°C for 1 and 2 h. The ensuing particles were monodispersed with a size distribution ranging from 5 to 10 nm. At room temperature, the particles were found to be superparamagnetic with negligible coercivities equal to 11-12 Oe. The saturation magnetization values were in the range of 20-25 emu/g. To render them water-soluble, the particles were functionalized with organic moieties.

The magnetic properties of powders can be substantially modified upon conformation and sintering. Thermal treatment can promote modification of the oxidation states on the metallic cations, altering significantly their magnetic behavior. On the other hand, pressing the powder and sintering enhances the dipolar interactions among the grains that can turn into variations of coercivity and remanence. Additionally, the final shape of the piece determines the shape anisotropy, that in the case of magnets with high saturation magnetization also governs the magnetic behavior of the magnet. Thus, a proper analysis of the magnetic behavior of the material requires the preparation and characterization of a sintered specimen. However, despite its interest, almost no studies have been devoted to their sintering. In the few works available, cobalt ferrite was sintered in conventional electric furnaces at high temperatures, about 1400°C [9,10]. Spark plasma sintering (SPS) at temperatures ranging from 700 to 1000°C was also used [34]. The abovementioned reports on the preparation of $CoFe_2O_4$ nanoparticles by microwave-assisted synthesis [29-33] do not include the sintering of the powders.

The application of microwave energy to the processing of various materials such as ceramics, metals and composites offers several advantages over conventional and non-conventional heating methods. These advantages include unique microstructure and properties, improved product yield, energy savings and reduction in manufacturing cost [35]. Microwave heating is fundamentally different from the conventional one in which thermal energy is delivered to the surface of the material by radiant and/or convection heating that is transferred to the bulk of the material via conduction and also, the non-conventional sintering technique as SPS, where it is possible to consolidate powder compacts by applying an on-off dc electric pulse. In contrast, microwave energy is delivered directly to the material through molecular interaction with the electromagnetic field. In ceramic materials, the high

temperatures required to fully densify ceramic powders result in large grain sizes due to Ostwald ripening when traditional sintering techniques are used. This makes it extremely difficult to obtain dense materials with nanometric and sub-micrometric grain sizes [36]. To overcome the problem of grain growth, microwave sintering has been proposed in the present work as an efficient technique for hindering the grain growth as well as producing a homogenous microstructure. Other benefits of microwave sintering over conventional sintering techniques include reduced cracking and thermal stress, increased strength and reduced contamination [37]. Microwave radiation for sintering of ceramic components has recently appeared as a newly focused scientific approach [38,39]. Recent works have proved the performance of the sintered materials either in rectangular [39] or cylindrical [40] cavities, providing really good mechanical properties [39,41].

The aim of the present work was to prepare nanoparticles of $CoFe_2O_4$ with high crystallinity and homogeneity by microwave-assisted hydrothermal synthesis through a systematic study of the influence of the microwave variables (temperature and reaction time) as well as of the use of different bases. A second objective was the preparation of dense ceramics of cobalt ferrite by microwave sintering of the nanopowder obtained with the best conditions. A final objective was the determination of the magnetic properties of both the nanopowders and the dense ceramic, in order to establish the possible use of this material as a permanent magnet.

2. Material and methods

2.1. Powder synthesis

2.1.1. Microwave oven

A commercial Milestone ETHOS 1 (Sorisole, Italy) microwave oven specifically designed for synthetic applications operating at 2450 MHz and capable of programming and adjusting the most important reaction parameters (power, temperature, pressure and time) was used. This multimode instrument features a built-in magnetic stirrer, automatic temperature and pressure control for direct monitoring of vessel content, and software that enables on-line temperature/pressure control by regulation of microwave power output. The multimode ETHOS 1 is equipped with two magnetrons. Installed power is 1600 Watts (800 Watts x 2), and delivered power is 1500 Watts in 1 Watt increments.

The magnetrons work in conjunction with a premixing chamber in the rear of the cavity where the output of the two magnetrons is combined, and a pyramid-shaped rotating microwave diffuser which ensures homogeneous microwave distribution throughout the entire cavity, preventing localized hot and cold spots.

The reactions were carried out in a 100 ml sealed vessel made of high-purity TFM, which is surrounded by a safety shield (made of HTC, a new high-performance plastic) and it includes a "vent-and-reseal" safety valve. Temperature and pressure during synthesis were monitored and controlled with the aid of a shielded thermocouple inserted directly into the vessel and with a pressure transducer sensor connected to the vessel. Built-in magnetic stirring (Teflon-coated stirring bar) was used. The evolution of time, temperature, pressure and power were continuously recorded during each experiment.

2 1.2. Chemicals

All chemical reagents in present work were of analytical grade and used as received without further purification. All aqueous solutions were prepared with deionized water with a resistivity of >18 MΩ cm, produced by a Milli-Q Plus pure water generating system from Millipore (Bedford, MA, USA).

$Fe(NO_3)_3 \cdot 9H_2O$ (Merck, Darmstadt, Germany), $Co(NO_3)_2 \cdot 6H_2O$ (Merck, Darmstadt, Germany), ammonium hydroxide solution (25%, 0.903 g cm^{-3} density, Merck, Darmstadt, Germany), and tetrapropylammonium hydroxide (TPAH) solution (1.0 M in H_2O, 1.012 g cm^{-3} density, Sigma-Aldrich, St. Louis, MO, USA) were used as starting materials.

Stock solutions ≈1M of $Fe(NO_3)_3 \cdot 9H_2O$ and $Co(NO_3)_2 \cdot 6H_2O$ were prepared, and they were standardized by Inductively Coupled Plasma Optical Emission Spectrometry (ICP-OES) by using a Iris Advantage Duo (Thermo Jarrell Ash, Waltham, MA, USA) spectrometer. For the standardization of both stock solutions, as well as for the determination of Co and Fe in the supernatant liquid, the calibration was performed with standard solutions of appropriate concentration prepared by serial dilution from standard stock solutions of 1.000±0.002 g l^{-1} of Fe and Co (Panreac, Barcelona, Spain). As analytical lines, the wavelengths at 259.939 nm of Fe and at 238.892 nm of Co were used.

2.1.3. Procedure

In a typical procedure to prepare $CoFe_2O_4$, 7 mmol of $Fe(NO_3)_3 \cdot 9H_2O$ (from standardized stock solution), 3.5 mmol of $Co(NO_3)_2 \cdot 6H_2O$ (from standardized stock solution) and 20 ml of H_2O were put into the 100 ml TFM vessel of the ETHOS 1 microwave oven, keeping a constant stirring. Under continuous

stirring, the base (NH_4OH or TPAH) was added dropwise until a pH of 9±0.2 was reached. Immediate formation of an orange-brown large colloidal solid was observed. The vessel was sealed and placed in the microwave oven, where it was heated to different temperatures (110, 130, 140, 160, 180, and 190°C) at a rate of 0.2°C s^{-1} and held at this temperature for 20 min. In the case of heating at 130°C, two additional syntheses were performed: in the first, a higher heating rate of 1°C s^{-1} was used, maintaining the dwell time of 20 min; in the second, a lower dwell time of 5 min was employed, maintaining the heating rate of 0.2°C s^{-1}. After cooling at room temperature, a black suspension was obtained. The separation of the solid from the liquid was performed by centrifugation. The particles, of black color, were collected, washed 3-4 times with deionized water, and finally dried overnight in air at 110°C. The dried material was crushed using an agate mortar and sieved through a 100 µm sieve. The supernatant liquid, which varies from colorless to pink color depending on microwave conditions, and the washing water were transferred to a 1000 ml volumetric flask and made up to volume with deionized water, and it was analyzed by ICP-OES to determine the Co and Fe content as explained in the previous section.

2.2. Thermal treatments

2.2.1. Calcination

A portion of the powder obtained at 130°C using NH_4OH and heating rate/dwell time of 0.2°C s^{-1}/20 min was calcined at 500°C in air for 2 h at a heating rate of 2°C min^{-1}. The dried material was crushed using an agate mortar and sieved through a 100 µm sieve.

2.2.2. Microwave furnace for sintering

Microwave sintering of samples was performed in an experimental microwave system with a 2.45 GHz frequency, 1 kW magnetron and the TE_{101} cavity, and a motorized short-circuit to tune the cavity and connected to a laptop to allow an automatic tuning system [39]. The rectangular cavity excite in the TE_{101} mode, based on a WR-340 waveguide through a circular iris to maximize the Hx magnetic component of the TE_{101} mode. The sample is introduced in the cavity through an insertion hole located just in the center of the cavity and on the top of it. The insertion hole has a diameter of 3 cm to guarantee that the insertion hole is under cut-off and no microwave energy leakage through it with the TE_{11} mode, which is the fundamental mode in the cylindrical waveguide. In the center of the cavity the excited mode has a maximum of E_y component, and a behavior of a $\sin(\cdot)^2$ in the axial component and no variation in

the vertical component, which guarantees the homogeneity of the field in the sample, which is supposed to be about 1 cm of diameter as maximum. To allocate the sample in the center, a quartz tube is used, which is transparent to the microwave energy and allows centering the sample. It also allows introducing different atmosphere (or even vacuum). To monitorize the temperature, an optical pyrometer (Optris GmbH, Berlin, Germany) is located on the top of cavity. This allows including a control system to automatize the heating process, based on a PID system.

Heating rate was controlled to 75°C min^{-1} and applied from room temperature to the sintering temperature by adjusting the position of the movable reflector between 100-400 W of power. The cooling stage was also controlled to 50°C min^{-1}. The maximum temperatures reached were 850°C and 900°C with a dwelling time of 10 min at the maximum temperature.

2.2.3. Powder sintering

Portions of the powder obtained at 190°C using NH_4OH and heating rate/dwell time of 0.2°C s^{-1}/20 min were uniaxially pressed at 200 MPa of pressure in a steel cylindrical die (2.5 mm thick, 10 mm Ø) and subsequently sintered in the microwave device at 850 and 900°C with a 10 min of dwelling time at the maximum temperature.

2.3. Characterization techniques

The crystalline phases of the as-synthesized and calcined powders, as well as of the sintered samples, were determined by X-ray diffraction (XRD) on a D8 Advance (Bruker, Karlsruhe, Germany) diffractometer using Cu K_α radiation. The measurements were performed in the 20°-70° range, and the step size and time of reading were 0.02° and 2 s, respectively. The XRD pattern of cobalt ferrite (PDF 22-1086) collected at the ICDD© databank (JCPDS-The International Centre for Diffraction Data©, Newton Square, PA, USA) was used as references for the analysis of our XRD patterns.

As-prepared powders, sintered bodies and fresh fracture surfaces were characterized by field emission scanning electron microscopy (FE-SEM) on a S-4800 type I (Hitachi, Tokyo, Japan) microscope.

As-synthesized powders were also observed by transmission electron microscopy (TEM) on a H-7100 (Hitachi, Tokyo, Japan) microscope working at 125 keV and by high-resolution transmission electron microscopy (HR-TEM) on a JEM-2100F (JEOL, Tokyo, Japan) microscope working at 200 keV.

The bulk density of the sintered samples was measured by Archimedes' principle by immersion in water.

2.4. Magnetic properties

Magnetization curves at low temperature (4 K) and at room temperature of the as-synthesized and calcined powders, as well as of the sintered samples, were measured in the range from −50 kOe to +50 kOe using a superconducting quantum interference device (SQUID) from Quantum Design (USA). Thermal dependence of the magnetizations was also measured in Zero Field Cooling (ZFC) and Field Cooling (FC) runs by applying a cooling field of Hcooling = 50 kOe and a magnetic field of Hmeas = 50 Oe during the measurement.

3. Results and Discussion

3.1. Powder synthesis

In the proposed synthesis, the general chemical reaction takes place in two steps. In the first step, the precipitation of Fe and Co hydroxides occurs according to the following equation (when NH_4OH is used as the base):

$$2\ Fe(NO_3)_3{\cdot}9H_2O + Co(NO_3)_2{\cdot}6H_2O + 8\ NH_4OH \rightarrow 2\ Fe(OH)_3\downarrow + Co(OH)_2\downarrow + 8NH_4NO_3 + 24\ H_2O$$

In the second step, the dehydration of hydroxides by microwave heating leads to the formation of cobalt ferrite, according to the following equation:

$$2\ Fe(OH)_3\downarrow + Co(OH)_2\downarrow \rightarrow CoFe_2O_4\downarrow + 4\ H_2O$$

$Fe(NO_3)_3{\cdot}9H_2O$ is a compound with a melting point of 47°C which decomposes at ca. 100°C with elimination of water of crystallization. $Co(NO_3)_2{\cdot}6H2O$ is a compound with a melting point of 57°C which decomposes at ca. 74°C with elimination of water of crystallization. Consequently, the compounds

cannot be dried to eliminate moisture, so it is very difficult to quantitatively weigh an accurate quantity of both products. Because of this, stock solutions of both $Fe(NO_3)_3 \cdot 9H_2O$ and $Co(NO_3)_2 \cdot 6H_2O$ were prepared with a concentration approximately 1M, in order to add to the vessel about 10.5 ml (volume range in the vessel is 8-50 ml), and they were standardized by ICP-OES. That ensures the use of stoichiometric amounts of Fe and Co.

However, after the completion of microwave-assisted synthesis, the supernatant liquid had a variable color, from colorless to pink color depending on microwave conditions. As this pink color can be explained by the presence of Co in solution (as Co^{2+} or, most likely, as pointed out by Silva et al. [42], as soluble amino complexes of Co) the content of this element (and also of Fe) in the supernatant liquid was determined by ICP-OES, and the results are shown in the next section.

The global time of the microwave-assisted hydrothermal synthetic procedure is lower than 1 hour (7-14 min for heating from RT to 110-190°C, 20 min of dwell time, and ≈20 min for cooling to RT). The pressure reached during heating was in the range of 2.6±0.1 bar (heating at 110°C) to 13.4± 0.1 bar (heating at 190°C).

3.2. Stoichiometry of the synthesized $CoFe_2O_4$

The analytical determination by ICP-OES of Fe in the supernatant liquids for all microwave conditions showed that the concentration of this element was below its quantification limit (QL, about 1 μg ml^{-1}). This means that the content of Fe in the supernatant liquids was lower than 100 μg, corresponding to 0.0018 mmol $Fe(NO_3)_3 \cdot 9H_2O$, which verified the quantitative precipitation (higher than 99.97%) of this element.

However, the behavior of Co is quite different. Its determination by ICP-OES in the supernatant liquids showed that the concentration of this element was below its QL (about 1 μg ml^{-1}, as for Fe) only for some microwave conditions. In these cases, the content of Co in the supernatant liquids was lower than 100 μg, corresponding to 0.0017 mmol $Co(NO_3)_2 \cdot 6H_2O$, which confirmed the quantitative precipitation (higher than 99.95%) of this element. Fig. 1 shows the Co content (in weight % with respect to the starting Co) in supernatant liquids for all syntheses carried out. As can be seen in Fig. 1a, the higher the reaction temperature, the lower the Co content. Only at 190°C the quantitative precipitation of Co occurs. The effect of the heating rate and the reaction time can be observed in Fig. 1b, where it is evident that a higher heating rate or, mainly, a lower reaction time leads to high levels of Co in solution (until

7%). The influence of the use of TPAH instead of NH_4OH is illustrated in Fig. 1c, which shows that the use of TPAH instead ammonia leads to a concentration of Co the supernatant lower than the QL, which is consistent with the results obtained by Paike et al. [17] in the synthesis of $CoFe_2O_4$ by coprecipitation using different tetraalkyl (*i.e.* tetramethyl, tetraethyl, and tetrabutyl) ammonium hydroxides as precipitating agents. Therefore, the quantitative precipitation of both Co and Fe elements occurs at the higher temperature of 190°C by using NH_4OH and at the lower temperature of 130°C by using TPAH, with a heating rate of 0.2°C s^{-1} and a reaction time of 20 min. Other authors who prepared cobalt ferrite powders by chemical routes, found Co-rich [16,20] and Fe-rich [43] compounds.

3.3. Crystalline phases

Representative XRD patterns of as-synthesized powders are shown in Fig. 2. The XRD patterns reveal that, in all cases, all peaks correspond to the characteristic peaks of standard structure of $CoFe_2O_4$, which has a cubic, spinel type lattice. This means that crystallization process has appeared even at the lowest reaction temperature of 110°C. The diffraction peaks are clearly broadened, which can be attributed to the small grain size. The absence of extra peaks evidence phase purity, even for Fe-rich samples (Figs. 2a, b, d and e). However, it can be observed some correlation between the stoichiometry of the compounds and their crystallinity: the higher the Co content in the supernatant (and, consequently, the lower the stoichiometry), the lower the crystallinity. For example, the compound obtained by using a temperature of 130°C and NH_4OH at heating rate of 0.2°C s^{-1} and dwell time of 5 min leads to broad and weak XRD peaks (Fig. 2e). On the contrary, the sample prepared at 190°C using NH_4OH (Fig. 2c) and, mainly, the sample synthesized at 130°C using TPAH (Fig. 2f) lead to more defined and sharper peaks. In other words, the XRD patterns show that peaks become sharper and stronger with the stoichiometry of the cobalt ferrite, indicating that the crystallization is becoming better and the average crystallite size is becoming bigger. On the other hand, diffraction pattern of the calcined powder (Fig. 2g) shows an improvement in peak intensities due to the increase in crystallinity and particle size.

3.4. Morphology

Fig. 3 and Fig. 4 show the FE-SEM and TEM images, respectively, of the two best samples, i.e., the samples synthesized by using NH_4OH at a temperature of 190°C and by using TPAH at a temperature of

130°C, with heating rate/dwell time of 0.2°C s^{-1}/20 min in both cases. As can be observed, the particles are very uniform in both shape and size, and possess nanosized spherical morphology. The particle sizes were determined from the TEM pictures to be about 5-10 nm.

As it is well-known, in conventional synthetic reactions, crystals are more likely to nucleate on container walls or dust particles, and suffer a slow growth rate because of very few crystal seeds and heating in an inhomogeneous mode. However, microwave heating presents a rapid heating to crystallization temperature due to the volumetric and homogeneous heating effects of microwaves, resulting in fast, simultaneous and homogeneous nucleation, crystal growth and development of massive seeds throughout the bulk solution. The seeds created under homogeneous conditions will lead to faster crystal growth, and the final products will have narrower size distributions and higher morphological uniformity. As a consequence, the round-shaped particles obtained present a high homogeneity in shape and size, as abovementioned.

The HRTEM images (Fig. 5) of the two best samples show that the nanoparticles are very similar in both cases, and confirm that the size of the nanoparticles is in the order of 5-10 nm. The micrographs, where lattice fringes are clearly observed, indicate that the nanoparticles are structurally uniform and have good crystallinity. In addition, these nanoparticles appear to be highly dispersed and without hard agglomerates.

3.5. Microwave sintered samples

The abovementioned powder was pressed into compacts for sintering tests. The green density was approximately 2.6 g cm^{-3}, i.e. 49% of theoretical density (5.30 g cm^{-3}). The relative density of $CoFe_2O_4$ ceramics sintered by microwave technique at 850 and 900°C was 97.6 and 98.2%, respectively. The density increases with the increase of microwave sintering temperature. This confirms that microwave sintering is a powerful route to obtain dense ceramics at lower temperatures and shorter cycles than those obtained by conventional sintering.

Fig. 6 shows the XRD pattern of $CoFe_2O_4$ ceramics sintered at 900°C by microwave technique. The XRD pattern of sample sintered at 850°C (not shown here) is similar. As expected, the main diffraction peaks correspond to the characteristic peaks of standard structure of $CoFe_2O_4$. Compared with XRD patterns of as-synthesized powders and of powder calcined at 500°C (Fig. 2), the diffraction patterns of the sintered samples show an improvement in peak intensities due to the increase in

crystallinity and particle size at the low sintering temperatures of 850 and 900°C. No secondary phases are detected in these XRD patterns.

FE-SEM images of microwave-sintered $CoFe_2O_4$ material are shown in Fig. 7, revealing a fine microstructure and high homogeneity at both temperatures. The average grain sizes of $CoFe_2O_4$ ceramics sintered by microwave at 850 and 900°C are 20-60 nm and 30-80 nm, respectively. This suggests a significant increase of grain size for a relatively low increase of density.

3.6. Magnetic properties

Fig. 8 shows the magnetization curves of the samples measured at 4K and 300K. As it can be observed at 4K all the magnetization curves exhibit a double hysteresis loop except that corresponding to the material sintered at 900°C. The composed magnetization curves have a main component with coercive fields ranging from 1.2 to 1.8 KOe depending on the sample processing parameters and a secondary component with coercive fields between 150 and 300 Oe. A numerical analysis estimates that this secondary component is responsible of about 10-15% of the magnetization of the material. Note that the sample annealed at 900°C lacks from the broad component.

It is well known that cobalt ferrite nanoparticles exhibit monodomain behavior for sizes smaller than ≈40 nm [44]. Below this size, magnetization reversal takes place by coherent spin rotation yielding coercive fields of the order of KOe. Above 40 nm, the nanoparticles present multidomain behavior and the inversion of magnetization is achieved by nucleation and motion of by domain walls leading to reduced coercive field of the order of hundreds of Oe. The micrographs of the samples above presented (Figs. 3, 4 and 5) exhibit a broad size distribution with nanoparticles diameter below 40 nm. Those particles are responsible of the main hysteresis loop with coercive fields of the order of few KOe.

Concerning to the secondary loop with reduced coercivity, it could be related to very small particles close to the superparamgnetic limit. However, FE-SEM, TEM and HR-TEM analysis did not show a bimodal size distribution that could account for the observed magnetization curves. Moreover, thermal dependence of the magnetization upon Filed-cooling and Zero-filed cooling did not show blocking temperatures up to 300^{o}C, so we can discard very small particles as responsible of the secondary loop. An alternative explanation could be that the secondary loop is associated with particles with modified stoichiometry in view of the fact that depending on the processing parameters there are defects of stoichiometry in the material as evidenced by the presence of Co in the supernatant liquid (Fig. 1).

However, we did not find a correlation between the intensity of the secondary loop and the deviation of the pure $CoFe_2O_4$ stoichiometry.

Finally, the reduced coercivity component could be due to agglomerates of monodomain nanoparticles. Agglomerates can lead to magnetostatic coupling between nanoparticles that reduce the energy barrier for magnetization reversal leading to smaller coercive fields [45,46]. Actually, it was recently found that $CoFe_2O_4$ nanoparticles coated with silica increase their coercivity because the silica shell reduces the magnetostatic dipolar interaction among the particles and a mixture of coated and uncoated nanoparticles lead to composed magnetization curves as those observed here [47]. The FE-SEM and TEM images of the material showed the presence of agglomerates as well as dispersed nanoparticles that can account for the observed hysteresis loops. A conglomerate of monodomain napoparticles can be also interpreted as a kind of a larger multidomain nanoparticle. Therefore, samples that are conformed only by larger multidomain nanoparticles should exhibit only low coercive components. Certainly, this is the case for the sample sintered at 900°C that with grains fairly larger than over 50 nm in the multidomain regime, only renders single hysteresis loops with low coercive field (Fig. 8). Therefore, this latter explanation seems to be at the origin of the low coercive field contributions and explains all our observations.

The magnetization curves at 300 K exhibit a very similar shape irrespective of the processing parameters. No double loops are observed and the coercivities of all the samples are below 150 Oe. This dramatic reduction of the coercivity is the result of the combination of two factors. On the one hand, the magnetocrystalline anisotropy constant of cobalt ferrite is strongly reduced with temperature [48]. This effect is associated with deformation of the unit cell from cubic above 116K to near rhombohedral below this temperature [1], being this effect particularly important for nanoparticles [49,50]. On the other hand, for magnetic nanoparticles, as the temperature increases and approaches to the blocking temperature the coercive field is reduced following a well established law [51] and the shape of the hysteresis loops approaches to the Langevin function.

Another important point of the magnetic properties analysis is the large variation in the saturation magnetization (M_S) that at 4 K ranges between 45 and 88 emu/g depending on the processing conditions. Fig. 9 summarizes the values of M_S of the samples. For the samples prepared using NH_4OH as the base, it can be seen that the saturation magnetization strongly increases with the synthesis temperature. Rising this temperature from 130°C to 190°C, the M_S increases at about 50%. As can be observed in Fig. 1, for synthesis conducted at lower temperatures (110-130°C), about 2% of the Co remains in the supernatant liquid, indicating a lack of Co in the nanoparticles that modifies their

stoichiometry. As the temperature increases the Co in the solution reduces and at 190°C there is no Co in the supernatant liquid. It is well known that modification of the stoichiometry in ferrite spinels induced important variations in the magnetic properties, and in particular in the M_S [19]. Cobalt ferrite is a ferrimagnetic spinel with two magnetic sub-lattices corresponding to A and B sites that are antiferromagnetically coupled. The saturation magnetization of the materials is the difference between those of the sub-lattices ($M=M_B-M_A$) [52]. Consequently, any defect of stoichiometry alters the magnetization of the sub-lattices yielding changes in the overall magnetization of the material. In particular, Co^{2+} ions occupy B sites and consequently a lack of Co reduces the magnetization of sub-lattice B and the net magnetization of the material.

Similarly, it can be observed that for the $CoFe_2O_4$ powder obtained at 130°C using TPAH as a base for the precipitation, the M_S of the material is fairly larger than that for the materials processed with the same parameters but using NH_4OH as base. According to Fig. 1, TPAH produces no Co in the supernatant liquid yielding to a material with the right stoichiometry while NH_4OH generates a lack of Co in the material of about 2%. This defect of stoichiometry justifies the difference in M_S as explained above.

4. Conclusions

It has been demonstrated that it is possible to obtain nanocrystalline (5-10 nm in size) cobalt ferrite powders by a one-pot microwave-assisted hydrothermal synthesis that is a simple, soft, fast, and energy efficient process without the need for catalysts or templates.

The microwave-assisted chemical route results in a better quality of cobalt ferrite because the mixing of the cations takes place at atomic level, which results in a very fine, dense, homogeneous and single-phase ferrite formation at lower temperature. The stoichiometry of the synthesized $CoFe_2O_4$ powders strongly depends on both the reagents used for precipitation (NH_4OH or TPAH) and the temperature of synthesis (heating rate and dwell time). Although both precipitating reagents lead to very similar nanopowders in morphology and size, the use of TPAH instead of NH_4OH allows a dramatic reduction in the temperature of synthesis from 190°C to only 130°C. In spite of this low temperature a high degree of crystallinity can be achieved by properly control the stoichiometry adjusting the synthesis parameters.

Sintered specimens with relative densities above 97.5% of theoretical can be achieved by a fast, non-conventional microwaves sintering process at temperatures of 850-900°C, much lower than that

obtained by conventional methods. The use of fast sintering allows maintaining small grain sizes, between 20-60 nm and 50-80 nm for sintering temperatures of 850 and 900°C, respectively, always in the nanometer size range.

The magnetic properties strongly depend on the final stoichiometry of the material, being optimum (i.e., maximum M_S) for the nominal $CoFe_2O_4$ composition. Such a composition can be tuned via the precursor used as a base and the annealing temperature. When TPAH is used as a base for the precipitation, the net magnetization of the sintered material is fairly larger than that of the materials processed with the same parameters but using NH_4OH as base due to the more accurate control of the stoichiometry associated to the lower Co dissolution observed in the synthesis with this base, probably associated to the lower synthesis temperature.

Acknowledgements

This work has been carried out with financial support from the Spanish Ministry of Economy, Industry and Competitiveness, MINECO, through the Project MAT2015-67586-C3-R. A. Borrell acknowledges the MINECO for her *Juan de la Cierva-Incorporación* contract (IJCI-2014-19839).

References

[1] H.P. Rooksby, B.T.M. Willis, Crystal structure and magnetic properties of cobalt ferrite at low temperatures, Nature 172 (1953)1054–1055.

[2] M.P. Sharrock, Particulate magnetic recording media: a review, IEEE Trans. Magn. 25 (1989) 4374–4389.

[3] H.M. Joshi, Y.P. Lin, M. Aslam, P.V. Prasad, E.A. Schultz-Sikma, R. Edelman, T. Meade, V.P. Dravid, Effects of shape and size of cobalt ferrite nanostructures on their MRI contrast and thermal activation, J. Phys. Chem. C 113 (2009) 17761–17767.

[4] J.P. Fortin, C. Wilhelm, J. Servais, C. Ménager, J.C. Bacri, F. Gazeau, Size-sorted anionic iron oxide nanomagnets as colloidal mediators for magnetic hyperthermia, J. Am. Chem. Soc. 129 (2007) 2628–2635.

[5] O.F. Caltun, G.S.N. Rao, K.H. Rao, B.P. Rao, C. Kim, C-O. Kim, I. Dumitru, N. Lupu, H. Chiriac, High magnetostrictive cobalt ferrite for sensor applications, Sensor Lett. 5 (2007) 45–47.

[6] O. Caltun, I. Dumitru, M. Feder, N. Lupu, H. Chiriac, Substituted cobalt ferrites for sensors applications , J. Magn. Magn. Mater. 320 (2008) e869–e873.

[7] I.C. Nlebedim, J.E. Snyder, A.J. Moses, D.C. Jiles, Dependence of the magnetic and magnetoelastic properties of cobalt ferrite on processing parameters, J. Magn. Magn. Mater. 322 (2010) 3938–3932.

[8] A.K. Giri, E.M. Kirkpatrick, P. Moongkhamklang, S.A. Majetich, V. G. Harris, Photomagnetism and structure in cobalt ferrite nanoparticles, Appl. Phys Lett. 80 (2002) 2341–2343.

[9] A. Rafferty, T. Prescott, D. Brabazon, Sintering behaviour of cobalt ferrite ceramic, Ceram. Int. 34 (2008) 15–21.

[10] S.D. Bhame, P.A. Joy, Effect of sintering conditions and microstructure on the magnetostrictive properties of cobalt ferrite, J. Am. Ceram. Soc., 91 (2008) 1976–1980.

[11] D. Zhang, X. Zhang, X. Ni, J. Song, H. Zheng, Synthesis and characterization of $CoFe_2O_4$ octahedrons via an EDTA-assisted route, J. Magn. Magn. Mater. 305 (2006) 68–70.

[12] P.D. Thang, G. Rijnders, D.H.A. Blank, Spinel cobalt ferrite by complexometric synthesis, J. Magn. Magn. Mater. 295 (2005) 251–256.

[13] S.H. Xiao, W.F. Jiang, L.Y. Li, X.J. Li, Low-temperature auto-combustion synthesis and magnetic properties of cobalt ferrite nanopowder, Mater. Chem. Phys. 106 (2007) 82–87.

[14] A.J. Rondinone, A.C.S. Samia, Z.J. Zhang, Superparamagnetic relaxation and magnetic anisotropy energy distribution in $CoFe_2O_4$ spinel ferrite nanocrystallites, J. Phys. Chem. B 103 (1999) 6876–6880.

[15] J-G. Lee, J.Y. Park, C.S. Kim, Growth of ultra-fine cobalt ferrite particles by a sol–gel method and their magnetic properties, J. Mater. Sci. 33 (1998) 3965–3968.

[16] T.A.S. Ferreira, J.C. Waerenborgh, M.H.R.M. Mendonça, M.R. Nunes, F.M. Costa, Structural and morphological characterization of $FeCo_2O_4$ and $CoFe_2O_4$ spinels prepared by a coprecipitation method, Solid State Sci. 5 (2003) 383–392.

[17] V.V. Paike, P.S. Niphadkar, V.V. Bokade, P.N. Joshi, Synthesis of spinel $CoFe_2O_4$ via the co-precipitation method using tetraalkyl ammonium hydroxides as precipitating agents, J. Am. Ceram. Soc., 90 (2007) 3009–3012.

[18] Q. Liu, J. Sun, H. Long, X. Sun, X. Zhong, Z. Xu, Hydrothermal synthesis of $CoFe_2O_4$ nanoplatelets and nanoparticles, Mater. Chem. Phys. 108 (2008) 269–273.

[19] L. Zhao, H. Zhang, Y. Xing, S. Song, S. Yu, W. Shi, X. Guo, J. Yang, Y. Lei, F. Cao, Studies on the magnetism of cobalt ferrite nanocrystals synthesized by hydrothermal method, J. Solid State Chem. 181 (2008) 245–252.

[20] L.J. Cote, A.S. Teja, A.P. Wilkinson, Z.J. Zhang, Continuous hydrothermal synthesis of $CoFe_2O_4$ nanoparticles, Fluid Phase Equilib. 210 (2003) 307–317.

[21] D. Zhao, X. Wu, H. Guan, E. Han, Study on supercritical hydrothermal synthesis of $CoFe_2O_4$ nanoparticles, J. Supercrit. Fluids 42 (2007) 226–233.

[22] S. Yáñez-Vilar, M. Sánchez-Andújar, C. Gómez-Aguirre, J. Mira, M.A. Señarís-Rodríguez, S. Castro-García, A simple solvothermal synthesis of MFe_2O_4 (*M* = Mn, Co and Ni) nanoparticles, J. Solid State Chem. 182 (2009) 2685–2690.

[23] L. Ajroudi, S. Villain, V. Madigou, N. Mliki, Ch. Leroux, Synthesis and microstructure of cobalt ferrite nanoparticles, J. Cryst. Growth 312 (2010) 2465–2471.

[24] K.J. Rao, B. Vaidhyanathan, M. Ganguli, P. A. Ramakrishnan, Synthesis of inorganic solids using microwaves, Chem. Mater. 11 (1999) 882–895.

[25] M. Nüchter, B. Ondruschka, W. Bonrath, A. Gum, Microwave assisted synthesis – a critical technology overview, Green Chem. 6 (2004) 128–141.

[26] B.A. Roberts, C.R. Strauss, Toward rapid, “green”, predictable microwave-assisted synthesis, Acc. Chem. Res. 38 (2005) 653-661.

[27] I. Bilecka, M. Niederberger, Microwave chemistry for inorganic nanomaterials, Nanoscale 2 (2010) 1358–1374.

[28] M. Baghbanzadeh, L. Carbone, P.D. Cozzoli, C.O. Kappe, Microwave-assisted synthesis of colloidal inorganic nanocrystals, Angew. Chem.-Int. Edit. 50 (2011) 11312–11359.

[29] S. Komarneni, M.C. D’Arrigo, C. Leonelli, G.C. Pellacani, H. Katsuki, Microwave-hydrothermal synthesis of nanophase ferrites, J. Am. Ceram. Soc. 81 (1998) 3041–3043.

[30] C-K. Kim, J-H. Lee, S. Katoh, R. Murakami, M. Yoshimura, Synthesis of Co-, Co-Zn and Ni-Zn ferrite powders by the microwave-hydrothermal method, Mater. Res. Bull. 36 (2001) 2241–2250.

[31] A.M. Ibrahim, M.M.A. El-Latif, M.M. Mahmoud, Synthesis and characterization of nano-sized cobalt ferrite prepared via polyol method using conventional and microwave heating techniques, J. Alloys Comp. 506 (2010) 201–204.

[32] F. Bensebaa, F. Zavaliche, P. L’Ecuyer, R.W. Cochrane, T. Veres, Microwave synthesis and characterization of Co–ferrite nanoparticles, J. Colloid Interface Sci. 277 (2004) 104–110.

[33] B. Baruwati, M.N. Nadagouda, R.S. Varma, Bulk synthesis of monodisperse ferrite nanoparticles at water–organic interfaces under conventional and microwave hydrothermal treatment and their surface functionalization, J. Phys. Chem. C 112 (2008) 18399–18404.

[34] N. Millot, S. Le Gallet, D. Aymes, F. Bernard, Y. Grin, Spark plasma sintering of cobalt ferrite nanopowders prepared by coprecipitation and hydrothermal synthesis, J. Eur. Ceram. Soc. 27 (2007) 921–926.

[35] W. H. Sutton, Microwave processing of ceramic materials, Am. Ceram. Soc. Bull. 68 (1989) 376–386.

[36] U. Anselmi-Tamburini, J.E. Garay, Z.A. Munir, Fast low-temperature consolidation of bulk nanometric ceramic materials, Scripta Mater. 54 (2006) 823–828.

[37] D. Michael P. Mingos, D.R. Baghurst, Applications of microwave dielectric heating effects to synthetic problems in chemistry, Chem. Soc. Rev. 20 (1991) 1–47.

[38] J. Binner, K. Annapoorani, A. Paul, I. Santacruz, B. Vaidhyanathan, Dense nanostructured zirconia by two stage conventional/hybrid microwave sintering, J. Eur. Ceram. Soc. 28 (2008) 973–977.

[39] A. Borrell, M.D. Salvador, E. Rayón, F.L. Peñaranda-Foix, Improvement of microstructural properties of 3Y-TZP materials by conventional and non-conventional sintering techniques, Ceram. Int. 38 (2012) 39–43.

[40] A. Guyon, S. Charmond, D. Bouvard, C.P. Carry, J.M. Chaix, Microwave sintering of nanometric ceramic powders in a single mode resonant cavity, in: J. Tao (Ed.), Microwave and RF Power Applications. 13th International Conference AMPERE Toulouse 2011, Cépaduès-Editions, Toulouse, France , 2011, pp. 237–240.

[41] R. Benavente, M.D. Salvador, O. García-Moreno, F.L. Peñaranda-Foix, J.M. Catalá-Civera, A. Borrell, Microwave, spark plasma and conventional sintering to obtain controlled thermal expansion β-eucryptite materials, Int. J. Appl. Ceram. Technol. 12 (2015) E187–E193.

[42] J.B. Silva, W. de Brito, N.D.S. Mohallem, Influence of heat treatment on cobalt ferrite ceramic powders, Mater. Sci. Eng. B 112 (2004) 182–187.

[43] L.B. Tahar, W. M'Nasri, L.S. Smiri, J.P. Quisefit, S. Ammar, Comparative study of the structural and magnetic properties of two cobalt ferrite nanocrystals produced with different iron precursors, Mater. Lett. 113 (2013) 198–201.

[44] C.N. Chinnasamy, B. Jeyadevan, K. Shinoda, K. Tohji, D.J. Djayaprawira, M. Takahashi, R.J. Joseyphus, A. Narayanasamy, Unusually high coercivity and critical single-domain size of nearly monodispersed $CoFe_2O_4$ nanoparticles, Appl. Phys. Lett., 83 (2003) 2862–2864.

[45] A.F. Gross, M.R. Diehl, K.C. Beverly, E.K. Richman, S.H. Tolbert, Controlling magnetic coupling between cobalt nanoparticles through nanoscale confinement in hexagonal mesoporous silica, J. Phys. Chem. B 107 (2003) 5475–5482.

[46] J.G. Barbosa, M.R. Pereira, J.A. Mendes, M.P. Proença, J.P. Araújo, B.G. Almeida, Cobalt ferrite thin films deposited by electrophoresis on p-doped Si substrates, J. Phys. Conf. Ser. 200 (2010) 072009.

[47] E. Girgis, M.M.S. Wahsh, A.G.M. Othman, L. Bandhu, K.V. Rao, Synthesis, magnetic and optical properties of core/shell $Co_{1-x}Zn_xFe_2O_4/SiO_2$ nanoparticles, Nanoscale Res. Lett. 6 (2011) 460.

[48] M. Tachiki, Origin of the magnetic anisotropy energy of cobalt ferrite, Prog. Theor. Phys. 23 (1960) 1055–1072.

[49] S. Yoon, Temperature dependence of magnetic anisotropy constant in cobalt ferrite nanoparticles, J. Magn. Magn. Mater. 324 (2012) 2620–2624.

[50]. S. Bhattacharyya, J-P. Salvetat, R. Fleurier, A. Husmann, T. Cacciaguerra, M.L. Saboungi, One step synthesis of highly crystalline and high coercive cobalt-ferrite nanocrystals, Chem. Commun. (2005) 4818–4820.

[51]. B.D. Cullity, C.D. Graham, Introduction to magnetic materials, second ed., Wiley, New Jersey, 2009, p. 383.

[52]. I.C. Nlebedim, A.J. Moses, D.C. Jiles, Non-stoichiometric cobalt ferrite, $Co_xFe_{3-x}O_4$(x=1.0 to 2.0): Structural, magnetic and magnetoelastic properties, J. Magn. Magn. Mater. 343 (2013) 49–54.

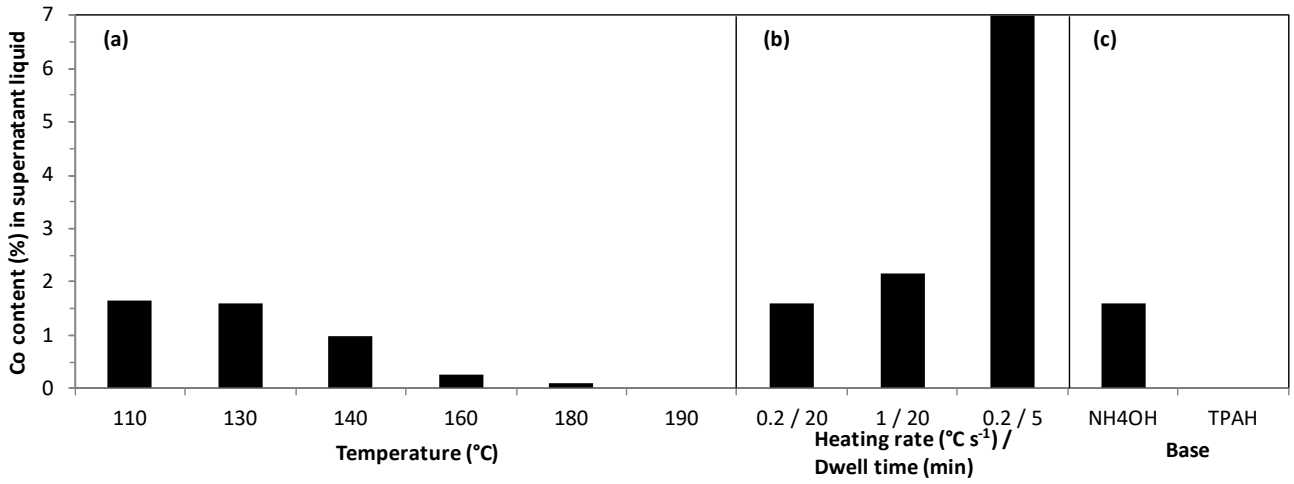

Fig. 1. Co content (in weight % with respect to the starting Co) in supernatant liquids as a function of (a) temperature of synthesis, using NH_4OH and heating rate/dwell time of 0.2°C s^{-1}/20 min, (b) heating rate and dwell time, using a temperature of 130°C and NH_4OH, and (c) the type of base, using a temperature of 130°C and heating rate/dwell time of 0.2°C s^{-1}/20 min.

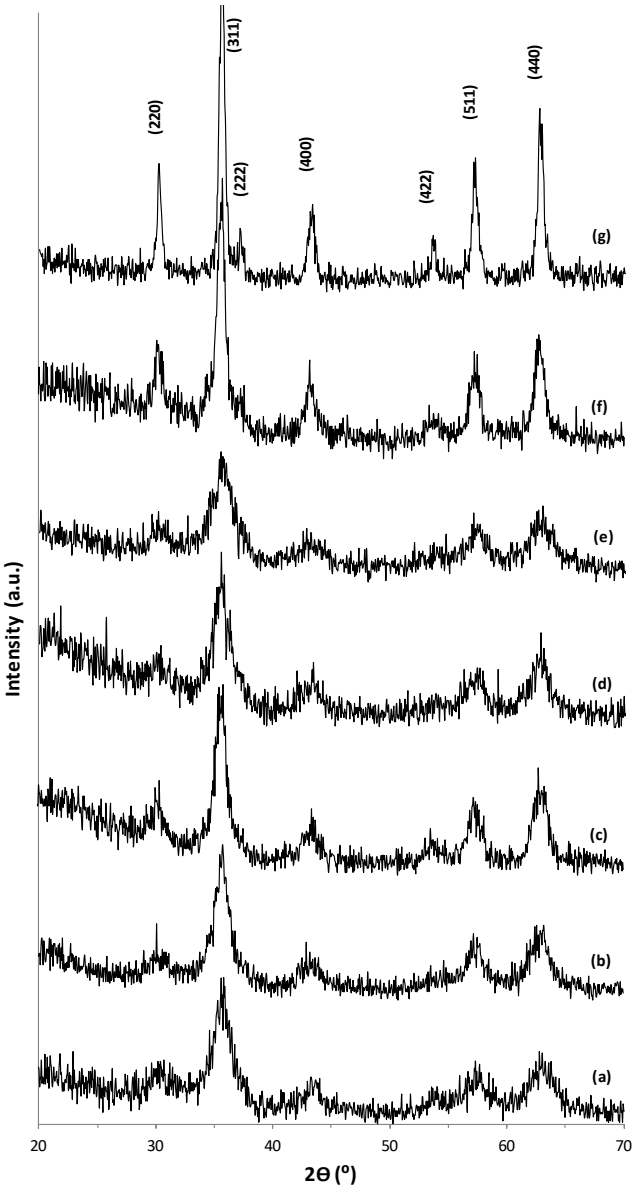

Fig. 2. XRD patterns of as-synthesized powders: using NH_4OH, heating rate/dwell time of 0.2°C s^{-1}/20 min at temperature of synthesis of (a) 110°C, (b) 130°C and (c) 190°C; using a temperature of 130°C and NH_4OH, at heating rate/dwell time of (d) 1°C s^{-1}/20 min and (e) 0.2°C s^{-1}/5 min; (f) using a temperature of 130°C, TPAH and heating rate/dwell time of 0.2°C s^{-1}/20 min; and (g) using NH_4OH, heating rate/dwell time of 0.2°C s^{-1}/20 min at temperature of synthesis of 130°C, calcined at 500°C for 2 hours.

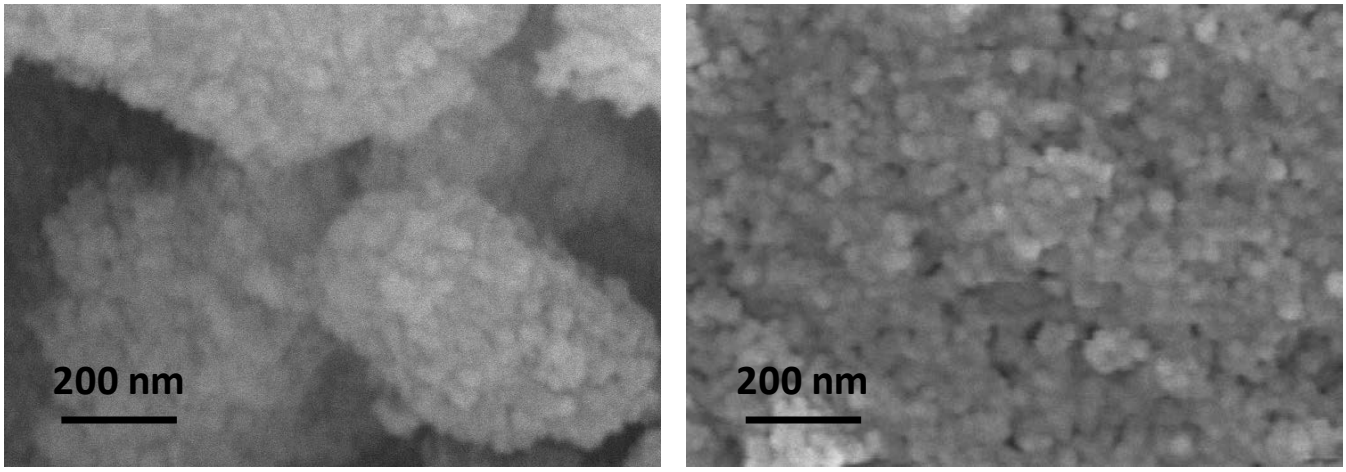

Fig. 3. FE-SEM images of as-synthesized $CoFe_2O_4$ powders using NH_4OH at temperature of synthesis of 190°C (left), and TPAH at temperature of synthesis of 130°C (right). The heating rate and dwell time were in both cases 0.2°C $s^{-1}$and 20 min, respectively.

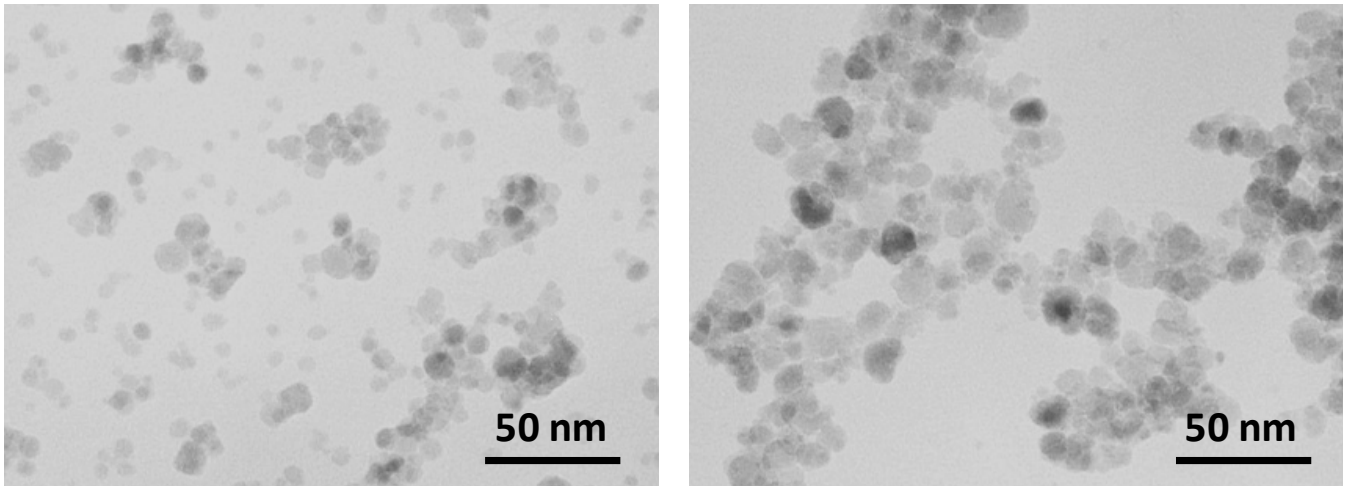

Fig. 4. TEM images of as-synthesized $CoFe_2O_4$ powders using NH_4OH at temperature of synthesis of 190°C (left), and TPAH at temperature of synthesis of 130°C (right). The heating rate and dwell time were in both cases 0.2°C $s^{-1}$and 20 min, respectively.

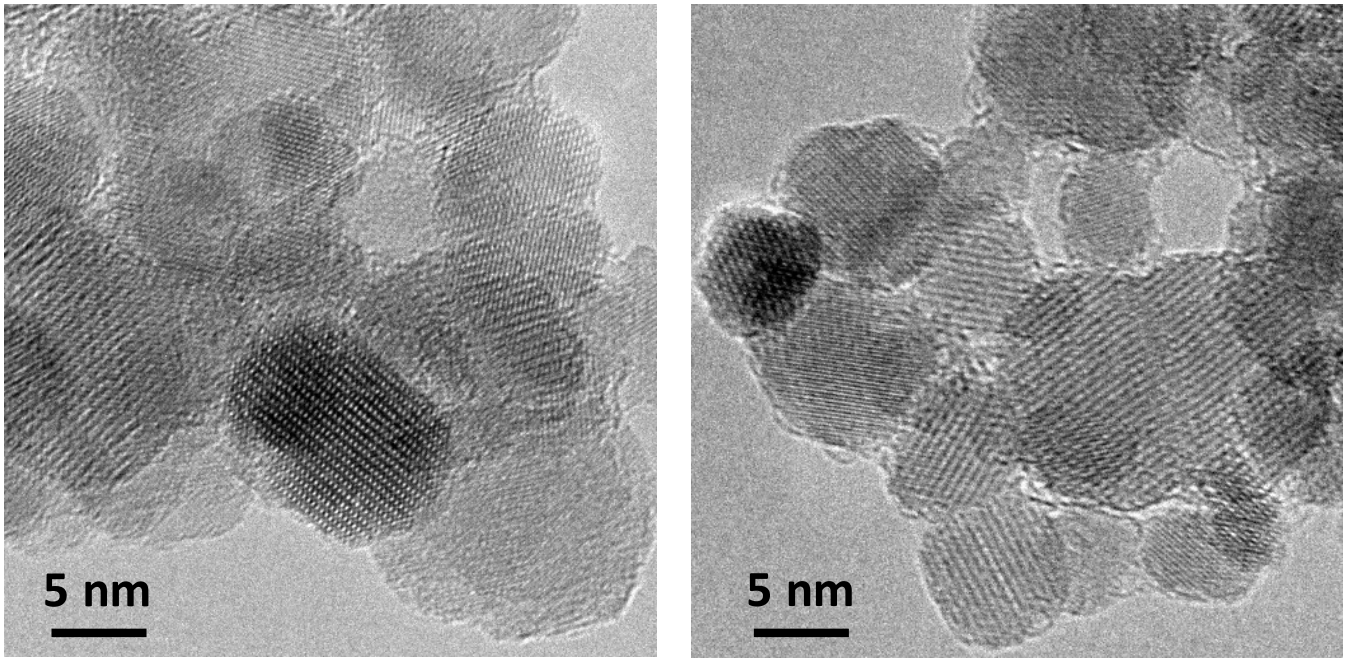

Fig. 5. HR-TEM images of as-synthesized $CoFe_2O_4$ powders using NH_4OH at temperature of synthesis of 190°C (left), and TPAH at temperature of synthesis of 130°C (right). The heating rate and dwell time were in both cases 0.2°C $s^{-1}$and 20 min, respectively.

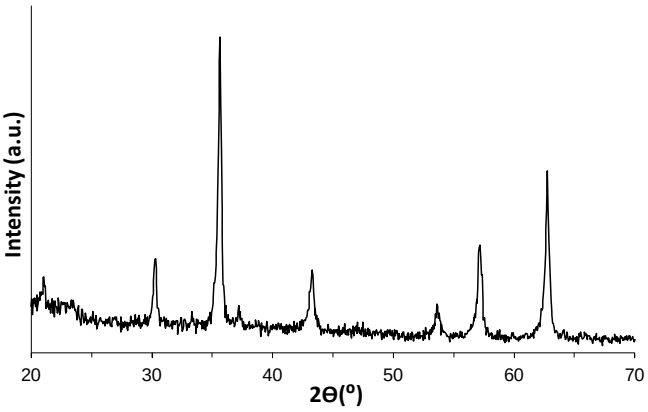

Fig. 6. XRD pattern of the $CoFe_2O_4$ powders obtained at 190°C using NH_4OH and heating rate/dwell time of 0.2°C s^{-1}/20 min, and sintered at 900°C for 10 min by microwave device.

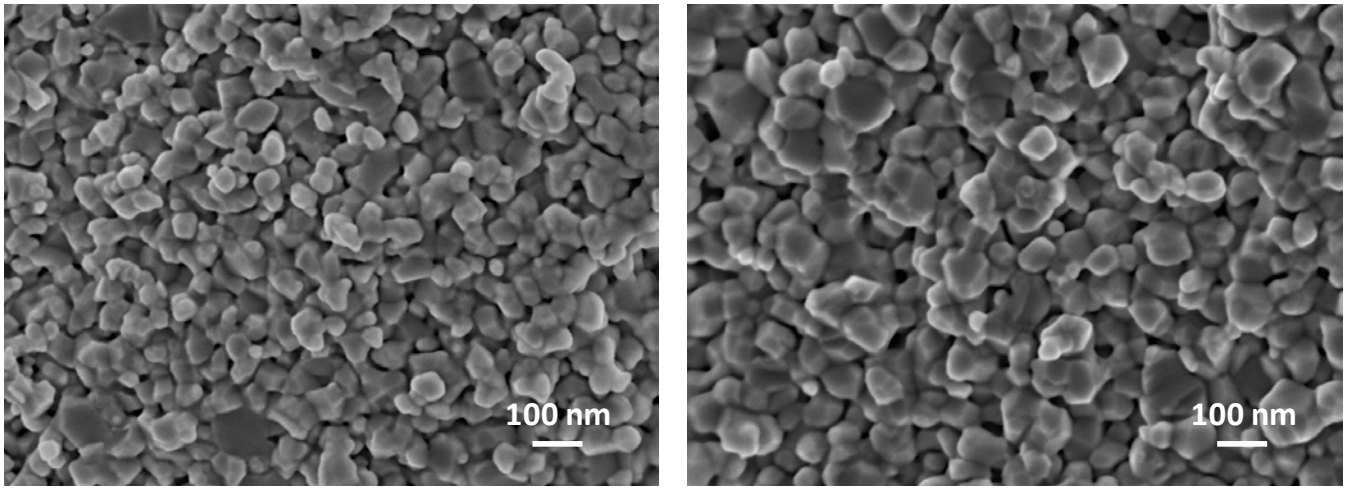

Fig. 7. FE-SEM images of the fresh fracture surfaces of $CoFe_2O_4$ samples obtained at 190°C using NH_4OH and heating rate/dwell time of 0.2°C s^{-1}/20 min, and sintered by microwave device for 10 min at 850°C (left) and 900°C (right).

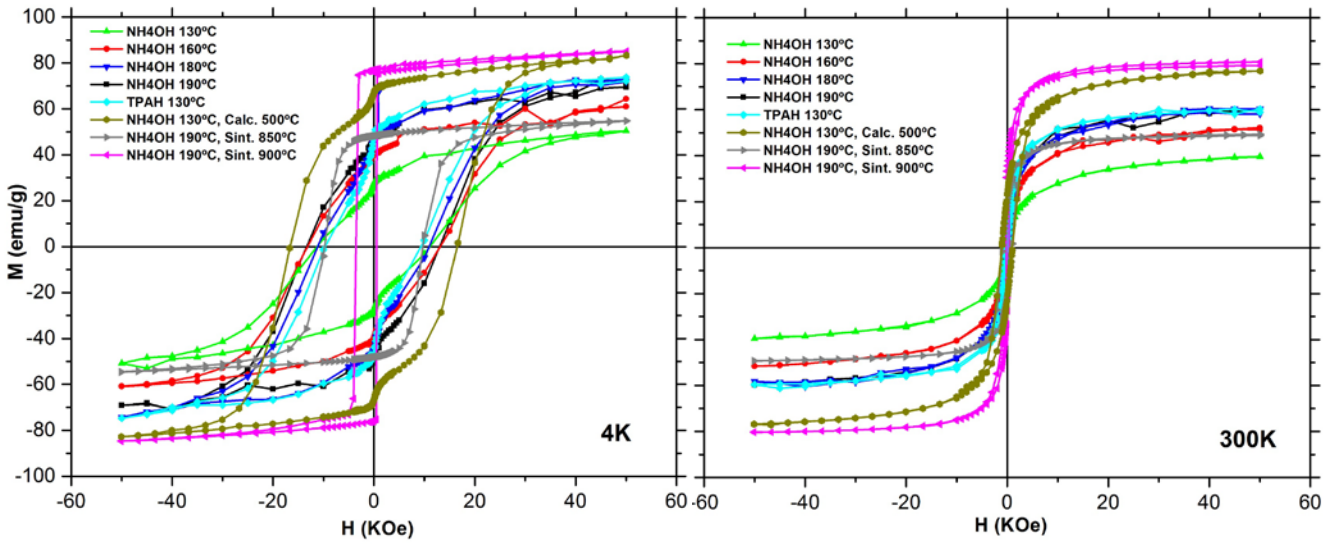

Fig. 8. Magnetization curves measured at (left) 4K and (right) 300 K of the samples prepared by microwave-assisted synthesis using NH_4OH at 130, 160, 180, and 190°C, TPAH at 130°C, NH_4OH at 130°C and calcined at 500°C for 2 hours, and NH_4OH at 190°C, and sintered at 850 and 900°C for 10 min. The heating rate and dwell time were in all cases 0.2°C s^{-1} and 20 min, respectively.

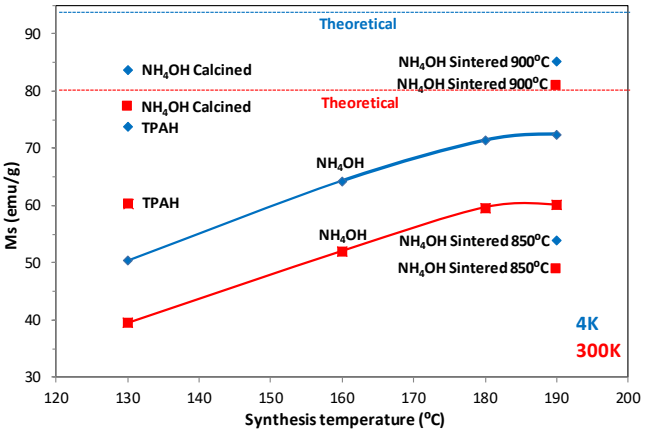

Fig. 9. Saturation magnetization at 4K and 300K of the different samples (summarized at the foot of Fig. 8) as a function of the temperature of synthesis, base used for precipitation and calcination and sintering treatments.